Topological simulations of dynamical features in coarsening soap froth

Boris Levitan and Eytan Domany
Department of Physics of Complex Systems, Weizmann Institute of Science, 76 100 Rehovot, Israel
(Received 15 November 1995; revised manuscript received 25 April 1996)

Simulations performed using a recently introduced deterministic topological model do not agree with some very recent results concerning the evolution of a single perturbed cluster. We analyze the source of the discrepancy and introduce a topological model that is in very good agreement with experiments and simulations available up to now. [S1063-651X(96)08309-2]

PACS number(s): 82.70.Rr, 02.50.−r, 05.70.Ln

I. INTRODUCTION

During the last decade there has been a surge of interest in the properties of two dimensional (2D) cellular structures [1]. This name refers to a wide variety of different physical systems, whose geometrical structure consists of a tiling of the plane by polygonal domains. One example of a cellular structure, which has attracted considerable attention of physicists recently, is soap froth confined between two parallel glass plates [2–6], such that thin soap films form a branched structure and the bubbles have the form of polygons. The cellular structure formed by the 2D soap froth evolves slowly with time. Since the soap froth is created in a nonequilibrium way, the gas pressure varies from bubble to bubble. The walls are penetrable for the gas; the pressure difference provides a slow diffusive flux between neighbor bubbles. This is the driving mechanism for the evolution of the soap froth.

Geometrical constraints have a considerable effect on the froth's evolution. The froth is made of thin soap films which are the bubbles' walls, that meet at vertices. The resulting 2D graph or film network has the following properties: First, only *three* edges can meet at a vertex; the fixed coordination number implies a strong geometrical constraint, originating from Euler's theorem, that relates N_b, the number of the bubbles in the system, to the number of the edges: $N_e=6N_b$. Hence the mean number of sides of a bubble is 6. Second, all the contact angles at a vertex are 120°. Diffusion of the gas between neighboring bubbles restricted by these two geometrical properties of the network leads to the *exact* von Neumann law of the dynamics of 2D soap froths [7], that relates the rate of area change of any bubble to the number of its sides (or ''topological class''), n:

$$\frac{da_n}{dt}=k(n-6). \tag{1}$$

As one can see immediately from this equation, bubbles with $n>6$ grow, while those with $n<6$ shrink and finally disappear. Since no new bubbles can be created and some disappear as a result of evolution, the total number of bubbles in the sample decreases. Since the total area of the bubbles (which is equal to the area of the sample) remains the same all the time, the mean area of a bubble, $\overline{a}$, grows in the course of the evolution.

After a transient period, this coarsening process leads to a scaling state. In this regime the mean area of the bubble grows linearly with time $\overline{a(t)}\sim t$ [and consequently, the number of bubbles $N(t)\sim t^{-1}$]. By scaling one means that two photographs of the system taken at different times differ only by an overall scale of all areas. When rescaled in units of $\overline{a}$, these two photographs become statistically identical; that is, *no statistical measurement can distinguish between the earlier and the later pictures*. In particular, the distribution of the areas and the topological classes, $F_n(a,t)$, is known to have the following scaling form:

$$F_n(a,t)=\frac{1}{\overline{a}}f_n(a/\overline{a}). \tag{2}$$

While theoretical and experimental research concentrated mainly on investigation of different properties of the scaling state, some work was devoted also to the transient behavior starting from initial states of the froth that in some sense were far from the scaling state. One of the simplest techniques to study soap froth dynamics in the scaling state as well as during the transient period approaching it is that of *topological simulations*. In Sec. II we describe various topological models, their successes and failures. The simplest topological model (model A) fails to provide agreement with three experiments (real and computer generated). The first is the *survivors' problem* [8]; the second concerns the approach to the scaling regime from a partially ordered initial state [9]. These two problems were remedied by introduction of model B [9]; however, recent computer experiments, which addressed the evolution of an ordered initial state with a *single defect* [10] disagreed with the predictions of this model. In Sec. III we identify the source of this discrepancy and present model C, a slightly modified version of B, which does agree with the single-defect experiments.

II. TOPOLOGICAL MODELS: SUCCESSES AND FAILURES

Let us turn now to modeling of the soap froth's evolution. Had the bubbles never changed their topological classes, Eq. (1) would have implied that after a short time only cells with $n>5$ remain in the froth, contradicting the geometrical constraint $N_e=6N_b$. However, when a bubble disappears, its neighbors undergo *topological rearrangements* (so called T2 processes) and change their topological classes. This way the

mean coordination number remains fixed. Since the von Neumann law describes the dynamics of the soap froth in terms of the areas and topological classes of the bubbles (topological approach), one could try to model the system using only these variables. A significant obstacle to such modeling is the fact that the outcome of the topological rearrangements is not unique: while a triangle disappears in a unique way, there are two possible ways for a rectangle and five for a pentagon. Which of these ''channels'' will be realized in each particular case depends on the geometrical configuration of the froth just before the bubble vanishes. Thus, in order to get an exact description, one should take into account the configuration of the froth explicitly.

On the other hand, models [11–16] that follow *all* details of the froth (simulate the motion of the walls) are numerically difficult to implement, especially for systems with a high number of bubbles. If one wishes to arrive at the scaling state with a large enough number of bubbles to make meaningful statistical measurements, some sort of reduced representation of the dynamics is helpful. Topological models, that keep only the areas of the bubbles and the topology of the network, do provide a reasonably simple representation. All such models must contain, however, a guess of how to choose the proper rearrangement T2 channel when a bubble disappears.

The simplest choice that can be made is selecting one of the channels at random [17,18]. Once this assumption has been made, one can describe the soap froth in terms of the areas of the bubbles and the topological connectivity of the bubble array, which is uniquely defined by the so-called *adjacency matrix* that identifies the neighbors of each bubble. One solves explicitly von Neumann's equations on a geometrically realistic *network* of bubbles [8,10,17,18] until the first one disappears (reaches $a_i=0$). At this point a T2 channel is selected at random, the neighbor cells change their topological classes, and the adjacency matrix also changes (we call the resulting model A).

Using model A one can solve very efficiently the dynamics of a very large number of bubbles. In spite of its relative simplicity (in comparison with the more elaborate calculations, such as for example, Refs. [11–15] that we do not describe here), the results can still be characterized as qualitatively correct. For some time this model was the best in the class of simple models of the soap froth and there was no indication that it is possible to improve it significantly without losing its simplicity.

Recently, however, *three* cases were found for which model A obviously disagreed with experiments. This has encouraged attempts to modify the model [9]. Let us briefly describe these three problems.

(i) The survivors' problem [8]; consider photos of the evolving froth, taken in the scaling state, at two subsequent times t_i and t_f, with $t_i<t_f$. Let the number of cells in these two pictures be $N(t_i)$ and $N(t_f)$, respectively $[N(t_i)>N(t_f)]$. Using the information about all the intermediate states of the froth, we can identify on the earlier picture (taken at t_i) each of the $N(t_f)$ cells that are present also in the latter picture. These cells differ from the remaining $N(t_i)-N(t_f)$ cells of the earlier picture in that all $N(t_f)$ survived till the moment t_f, while the others have disappeared before t_f. We call these $N(t_f)$ cells ''survivors'' while the name ''bubbles'' will be reserved for the others.

Obviously, the survivors' statistics differs from that of the entire ensemble of bubbles and it provides a dynamical characteristic of the scaling state, dealing with temporal correlations. Dependence of y_n, the topological class distribution of the survivors on time $(t=t_f/t_i)$, was investigated experimentally, by topological simulations and mean field calculations [8]; the main result was that the survivors' topological distribution approaches a fixed form in the long time limit. At the same time, as shown in Ref. [8], there is a strong *quantitative* disagreement between the experiment, mean field treatment, and topological simulations. (Note that the topological model used for simulations in Ref. [8] was different from model A considered here; however, later we repeated the same simulation using model A and found that there is almost no difference between the results of the two models.)

(ii) The second failure of model A is the behavior of the froth in the transient regime, when the initial state of the bubbles is a nearly ordered array of hexagons. The degree of disorder can be characterized by μ_2, the value of the second moment of the topological distribution of the froth. For an ordered state μ_2 is small (proportional to the density of the defects in the hexagonal structure of the bubbles array). At the scaling state it approaches some value $\mu_2\rightarrow\mu_2^{\rm sc}$. As long as the froth becomes more and more disordered in the course of the evolution, one would expect μ_2 to become larger and larger until it achieves its final value $\mu_2^{\rm sc}$. A remarkable feature of the transient period, contrary to the simple expectations, is a *pronounced peak* in the time dependence of $\mu_2(t)$. This has been observed in experiments by Stavans and Glazier [4], as well as in the numerical simulations of Weaire and Lei [19]. However, model A shows perfectly monotonic growth of $\mu_2(t)$ [9].

(iii) The third problem concerns growth of a single cluster [10]. The elementary ''unit'' of the transient behavior discussed above is the evolution of a single defect, such as one created by a single T1 switch on the ideal hexagonal network. Were it not for the defect, the ideal hexagonal network would have been stationary (as a consequence of the von Neumann law). So, our network consists of two parts: the evolving neighborhood of the defect (called cluster) and all the rest (the ideal hexagonal part), which does not evolve. Simulations of the single cluster growth by model A show that the topological distribution of the bubbles in the cluster approaches a steady form; its width is characterized by its second moment, $\mu_2=0.72$ (compare this with $\mu_2^{\rm sc}=1.2$ obtained by this model in the disordered scaling state).

When the single cluster dynamics was first addressed by the topological model A [10] there were no available experimental data on this problem. Very recently two independent numerical experiments were made. First is the simulation by Jiang, Mombach, and Glazier [20] of the Potts spin model [14]. Their initial configuration was an ideal network of hexagonal bubbles with a defect (a large 12-sided bubble surrounded by pentagons and hexagons) placed at the center. The results obtained in this work were in contradiction with the prediction of the topological model A [10]. They found that the well-developed cluster consists of one huge central bubble surrounded by a layer of small ones (mostly pentagons and hexagons). Such a structure of the cluster provides

in a trivial way an unbounded growth of the second moment, whereas model A predicts a fixed form of the topological distribution for the cluster and a finite value for μ_2.

We investigated whether this discrepancy is caused by the difference in the initial form of the defect, but found that even for the defect used in [20] the topological models give the same finite μ_2. Moreover, the result of the Potts simulations [20] was confirmed by Ruskin and Feng [21]. They simulated the model of Weaire and Kermode [11] with an initial defect of exactly the form used in [9,10]. These simulations also demonstrated unbounded growth of μ_2.

Thus model A fails to explain the results of these three problems. In order to determine the source of the failure of the topological approach, one has to reexamine the approximations involved in model A. Since it uses the exact von Neumann equations on a topologically correct network of cells, it describes this phase of the evolution exactly. Hence the only possible source of the failure is in the *random* way the T2 process is performed. A natural step is, therefore, to try to suggest more realistic rules for selecting the T2 process, that take into account the details of the bubbles' configuration. One wishes, however, to keep the model as simple as possible. Such a modification, introduced in Ref. [9], was based on the following rule: *in a T2 process the shortest side undergoes first a T1 switch*, turning a disappearing pentagon into a rectangle, which again executes a T1 switch of its shortest edge and turns into a triangle, which disappears in a single step by shrinking to a point. (A somewhat similar idea was proposed by Marder [22] in the frame of the mean field ''kinetic equation.'')

In order to implement this idea in a *topological* model one should express the information about the lengths of the edges $L_{i,j}$, separating two neighboring cells i and j in terms of the areas of the bubbles and the adjacency matrix. Dimensional estimation of the perimeter and area of a *typical* n-sided bubble leads to the following relation [9]:

$$L_{i,j}=\frac{\sqrt{a_i}\sqrt{a_j}}{n_i n_j}. \tag{3}$$

This relation, together with the rule stated above, defines a topological model (model B) that takes into account the effects of the areas and topological classes of the neighboring bubbles on the result of a T2 process. Actually, (3) is merely a crude dimensional estimate. Nevertheless, as shown in [9], model B improves considerably the results for problems (i) and (ii) mentioned above, as compared with model A.

In the present work we have extended our previous simulations of the survivors' problem [9] by model B; we generated a system of 100 000 bubbles and performed about 45 000 preliminary T1 switches in order to get a distribution of the topological classes close to what we expect from the T2 dynamics. Then we let the system evolve according to the von Neumann law, performing the T2 processes according to (3). The scaling state was achieved with good accuracy when there were about 64 000 bubbles. At this point we numbered all the bubbles and started to follow the survivors. We found that the convergence to a fixed distribution is slower than it was in the framework of model A (for which a fixed topological class distribution of the survivors seemed to be obtained when the number of bubbles decreased from 15 000 to 436 [8]). In order to achieve the same level of stationarity for model B we had to follow the survivors from 64 000 until 300–400 bubbles were left in the system, i.e., nearly four times longer.

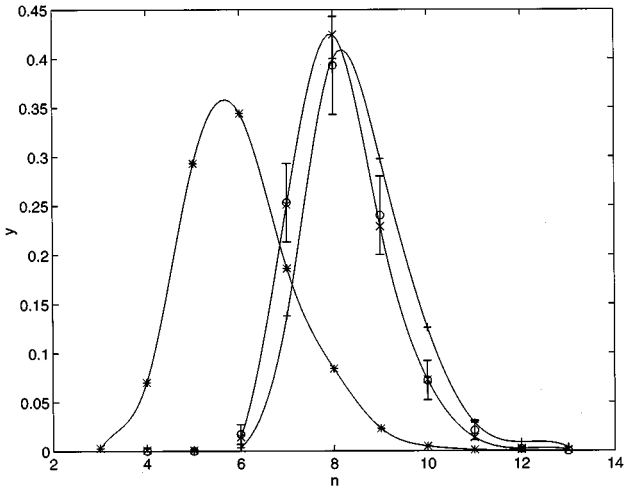

FIG. 1. The topological distribution of survivors obtained by simulations using model B. The initial configuration contained 64 000 bubbles. Two curves (marked by $\times$ and $+$, respectively) correspond to the moments when there were 2640 and 125 bubbles in the system. Circles represent the experimental points and stars denote the topological distribution in the (initial) scaling state. Notice that the experimental points are close to those obtained when there are 2640 bubbles in the system.

Our simulations are compared in Fig. 1 with the results of a previously reported experiment [8]. Evidently, the experimental data *do not* correspond to our calculated fixed shape of the distribution. Rather, we have very good agreement between the experimental points and one of our *intermediate* curves, corresponding to 2640 bubbles in the system, i.e., to reduction of the number of bubbles by a factor of about 24. This reduction is nearly the same as in the experiment, which started with $\sim$3000 and stopped at $\sim$120 bubbles. The definite distinction between the experimental distribution and the fixed limiting topological class distribution of our simulations may mean that the fixed form has not yet been achieved in the experiment.

In order to see clearly the dynamical behavior of the survivors' topological class distribution we present in Table I the relative fractions of n-sided survivors as a function of time (between the initial and the final pictures). Triangles were present in the scaling state but they were not observed among survivors even after a very short time and they do not appear in the table. Squares and pentagons disappear rather fast. The concentration of the hexagons (which are the major fraction in the scaling state) falls very quickly but it stabilizes when the number of bubbles is about 300 (reduction by factor 20). Analogously one can follow the evolution of each fraction in this table and be convinced that the significant y_l (i.e., $7 \leqslant l \leqslant 11$) stabilize when the number of bubbles is 300–400 (although y_{13} still grows even when $N=125$), while for $N=2400$ the distribution is still changing.

We turn now to the second problem mentioned above, the transient period of the froth evolution, starting from an initial configuration with small disorder. Using model B we did

TABLE I. Topological class distribution of survivors as a function of the number of bubbles in the system. The survivors are identified in the scaling state when the system contained 64 533 bubbles (i.e., the first line in this table represents the usual scaling distribution for all bubbles). Each new line corresponds to reduction of the number of bubbles by a factor of 1.5 compared to the previous line. All data were obtained by averaging over six runs to reduce fluctuations. The results of the experiment of Ref. [8] are also included (marked by ''Expt.'') for comparison.

N	$10y_4$	$10y_5$	y_6	y_7	y_8	y_9	y_{10}	y_{11}	$10y_{12}$	$10y_{13}$
64533	0.69	2.92	0.343	0.185	0.083	0.022	0.004	0.00073	0.0010	0.0000
42286	0.42	2.71	0.359	0.202	0.091	0.027	0.0062	0.00090	0.0011	0.0001
28012	0.00	0.754	0.430	0.304	0.137	0.041	0.0094	0.0014	0.0017	0.0002
18515	0.00	0.061	0.279	0.429	0.207	0.062	0.0140	0.0021	0.0025	0.0002
12295	0.00	0.004	0.119	0.470	0.293	0.092	0.021	0.0031	0.0038	0.0004
8168	0.00	0.001	0.049	0.418	0.364	0.131	0.032	0.0047	0.0057	0.0006
5432	0.00	0.000	0.024	0.347	0.403	0.171	0.045	0.0069	0.0086	0.0009
3609	0.00	0.000	0.016	0.287	0.419	0.206	0.060	0.0099	0.012	0.0014
Expt.	0.00	0.000	0.015± 10	0.25± 4	0.39± 5	0.24± 4	0.07± 2	0.025± 1	0.010± 5	0.0000
2396	0.00	0.000	0.013	0.240	0.424	0.233	0.075	0.013	0.015	0.0021
1592	0.00	0.001	0.008	0.213	0.421	0.250	0.088	0.016	0.019	0.0031
1055	0.00	0.000	0.007	0.191	0.417	0.265	0.097	0.019	0.024	0.0047
699	0.00	0.000	0.006	0.170	0.414	0.279	0.104	0.023	0.028	0.0071
462	0.00	0.000	0.005	0.149	0.421	0.279	0.115	0.026	0.036	0.0108
302	0.00	0.000	0.004	0.142	0.410	0.283	0.121	0.032	0.054	0.0166
195	0.00	0.000	0.004	0.133	0.421	0.284	0.117	0.031	0.076	0.0257
125	0.00	0.000	0.003	0.137	0.400	0.296	0.125	0.028	0.080	0.0269

obtain a peak of the second moment [9]. Moreover, the value of the second moment in the scaling regime, obtained from simulations of model B, $\mu_2^B=1.4$, was also in better agreement with the experimentally found $\mu_2=1.4\pm0.1$ than the result of model A, $\mu_2^A=1.2$.

In order to explain the slightly higher value of μ_2^B, we present in Table II the values for the ''control parameter'' $r=\sqrt{a}/n$ for bubbles with $n>5$ as obtained from averaging in the *scaling state*. First of all, we see that r does not vary too much and hence the random choice of equally probable T2 processes used by model A is quite justified (in the scaling regime) and does not cause as large a discrepancy as in the case of a single cluster. However, r does grow with n and it is especially small for pentagons and rectangles. Therefore as n increases, bubbles become less and less likely to lose sides and their lifetime increases. This leads to the following consequences.

(a) The fraction of many-sided bubbles is slightly greater in model B than in A, where the T2 processes were performed at random. This leads to the increase of the second moment from $\mu_2^A=1.2$ to $\mu_2^B=1.4$.

(b) The fixed distribution of the survivors is shifted to larger n, because now the many-sided bubbles have a higher chance to survive than within model A. The difference between these two models is more pronounced for the survivors' problem than for the scaling state because the overall topological distribution is constrained by the requirement $\overline{n}=6$, that is absent for the survivors' distribution.

In spite of the success of model B in reproducing the existence of the peak of μ_2 in the transient period as well as the properties of the survivors' dynamics as discussed above, it fails to reproduce the infinite growth of μ_2 in the single cluster problem. Simulations show that both models A and B give the same qualitative picture for a single cluster [9] (the distribution obtained by model B is slightly broader than that obtained by model A). Thus this crude discrepancy between the results of detailed numerical experiments and topological simulations shows that model B still leaves out some important feature of the T2 processes.

III. SIMULATING THE SINGLE CLUSTER EVOLUTION: MODEL C

What may still be missing in model B? The answer is probably contained in the papers by Fradkov and co-workers [23], who showed that the conditions of mechanical equilibrium in the soap froth are such that any four-sided bubble must be a perfect rectangle (i.e., with equal opposite sides) when it becomes much smaller than all its neighbors.

TABLE II. The mean areas of bubbles from various topological classes and the control ratio as a function of n, as calculated for model B. We used a short simulation, starting with 10 000 bubbles; the measurements were executed when the number of bubbles was between 2000 and 700.

n	4	5	6	7	8	9	10	11
$\overline{a_n}$	0.187	0.410	1.033	1.572	2.011	2.244	2.895	2.691
$\sqrt{\overline{a_n}}/n$	0.108	0.128	0.169	0.179	0.177	0.166	0.170	0.152

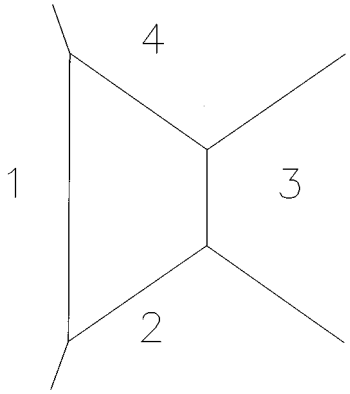

FIG. 2. Example of a bubble that *does not* satisfy the condition of mechanical equilibrium that requires opposite sides of a rectangle to be equal. Appearance of such an ''unphysical'' bubble in the simulations is allowed by model B. Model C, on the other hand, guarantees that disappearing rectangles behave as those for which conditions of mechanical equilibrium are fulfilled.

Clearly, calculating the lengths of the sides of a four-sided bubble by Eq. (3) we will never obtain a perfect rectangle.

This condition on disappearing rectangles is expected to be important only in situations such as the one illustrated in Fig. 2, where using Eq. (3) one identifies the maximal (''1'') and minimal (''3'') sides to be opposite while the maximal side is much longer than all the others. Then switching the minimal side, performed according to the rules of model B, ultimately leads to the smallest and the largest neighbors losing sides. It is intuitively clear that the bubble drawn in Fig. 2 is far from mechanical equilibrium. The result of the rearrangement would have changed if we had allowed the bubble to attain mechanical equilibrium before disappearing and take the form of a perfect rectangle with equal opposite sides (''1'' and ''3''). It is easy to modify the rules of model B so that disappearing four-sided bubbles behave as perfect rectangles. Using the same idea which led us to (3), we can do this in the following way.

Identify the two pairs of opposite sides (''1'', ''3'' and ''2'', ''4'') and compare $(\sqrt{a_1}/n_1)(\sqrt{a_3}/n_3)$ with $(\sqrt{a_2}/n_2)(\sqrt{a_4}/n_4)$. The pair for which this product is smaller is identified as that of smaller length, and each of these opposite sides will shrink to a point. Let us stress once again that this way of choosing the shortest side can play an important role (vs model B) only if the maximal side ''1'' is much larger than all the others.

Let us now consider the T2 process for a pentagon. According to Ref. [23], there is no constraint on the form of pentagons (unlike the four-sided bubbles). Therefore there is no reason to change in any way the rules for the first T1 process for pentagons. However, after losing a side a pentagon becomes four-sided. Although it is extremely small, it is subject to the same conditions of mechanical equilibrium as a usual four-sided bubble. Therefore the second T1 switch should be performed according to the general rule for such bubbles introduced above. Let us summarize the rules of our modified model (model C).

Pentagons: Perform one T1 switch of the minimal side [the lengths are calculated using (3)]; this step is exactly the same as in model B. The remaining four-sided bubble is then treated as a rectangle according to the rule below.

Rectangles: Find the two pairs of opposite sides, say, ''1''-''3'' and ''2''-''4''. For both pairs calculate the quantities $r_{i,j}=(\sqrt{a_i}/n_i)(\sqrt{a_j}/n_j)$. If $r_{1,3}>r_{2,4}$, the neighbors ''2'' and ''4'' will be those who lose a side, while the number of sides of ''1'' and ''3'' remains the same and, conversely, if $r_{1,3}<r_{2,4}$, then ''1'' and ''3'' will lose a side.

When this model C is used in our simulations, a single defect evolves into a cluster whose general form is very similar to that obtained in Refs. [20,21]. We observed mostly one large many-sided bubble in the center, surrounded mostly by pentagons, hexagons, and heptagons. Our simulations started with a defect prepared by a single T1 switch of the ideal lattice of hexagons and were stopped when one of the bubbles acquired more than 30 sides. We found that for different runs [24] starting with the same initial defect the final cluster sometimes contained only one large 30-sided bubble at its center (while all other bubbles have fewer than 20 sides), but we also had runs with three or four large bubbles (more than 22 sides). The total area of these large bubbles was about 3 times larger than the total area of all small surrounding bubbles in the cluster. The topological distribution of the small bubbles of the cluster was, however, quite similar in all these runs. This distribution was found to be somewhat different from the one calculated for the cluster presented in Ref. [21]. However, this is so because our data were obtained from larger clusters (of about 300 bubbles), while the cluster of Ref. [21] contains only 72 bubbles. When we calculated the topological class distribution for clusters of about 70 bubbles, rather good agreement with Ref. [21] was obtained, as shown in Table III.

Simulating the transient behavior for initial states with many isolated defects we found that $\mu_2(t)$ has a peak (see Fig. 3), whose magnitude depends strongly on the initial concentration of the defects: the smaller the concentration, the

TABLE III. Topological distribution of the cluster that evolves from a single defect. The first line presents data calculated for the cluster of Ref. [21]. That cluster contained 72 bubbles and was obtained from the same initial defect as used in our simulations. The second and the third lines correspond to our simulation using model C: obtained from ''small'' (70 bubbles) and ''large'' (about 400 bubbles) clusters, respectively. There is a reasonable agreement between the ''experiment'' [21] and our simulation, especially for statistically significant data (x_5 and x_6) taken from the small cluster.

n	5	6	7	8
x_n (Ref. [21])	0.167	0.628	0.057	0.029
x_n(small)	0.211	0.618	0.177	0.001
x_n(large)	0.277	0.532	0.100	0.026

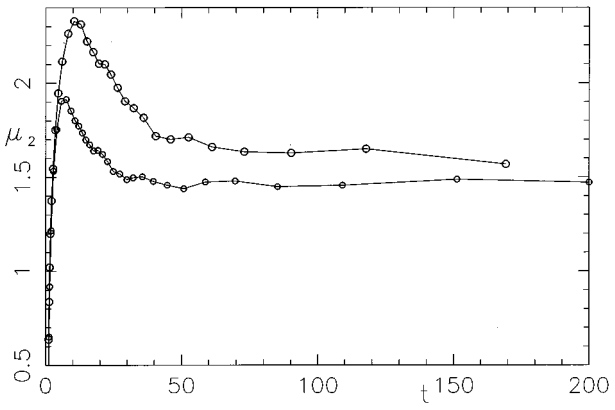

FIG. 3. The second moment of the topological distribution, μ_2, vs ''time'' $t=N_i/N$ ($N_i=40.000$ is the number of bubbles in initial configuration, N is the current number of bubbles in the system) as obtained from simulations of model C. Evolution from two ordered initial conditions, with defect densities $c=0.0125$ (upper curve) and $c=0.05$ (lower curve), is presented.

larger is the peak. The dependence of μ_2^{peak} on the initial concentration of defects, c, is shown in Fig. 4: at small c the growth of μ_2^{peak} seems to be unbounded [25]. At the same time, the peak obtained in simulations using model B has only a weak dependence on c, and for small c the magnitude of the peak is saturated.

These features follow directly from the behavior of a single cluster as described by the two models. Model B gives a finite value of the second moment μ_2^{cl}, so its value at the peak, μ_2^{peak} (corresponding to the state of the froth where all the initially present hexagons have just been transformed) is finite as well. In model C, μ_2^{cl} grows unbounded; therefore, if the initial density is small, i.e., the distance between the neighboring defects is large, at the moment when the clusters meet each other their second moment is consequently very large. Hence the value of μ_2^{peak} grows as the density decreases unbounded (this idea was expressed by Weaire before we obtained our results).

We tested this model also by simulating the properties of

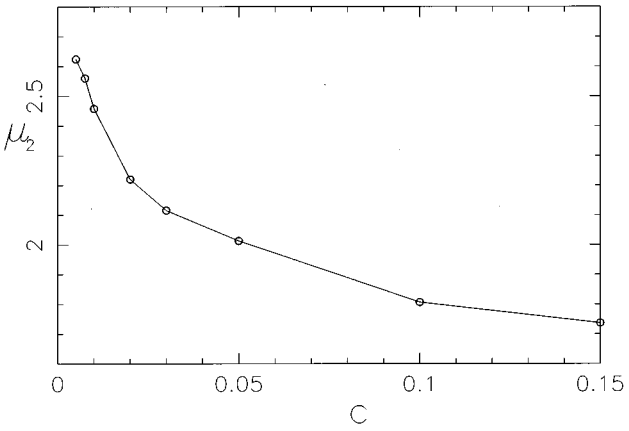

FIG. 4. Peak value of the second moment of the topological distribution during the transient period, μ_2^{peak} as a function of the initial density of defects, c. Each point is found by averaging over a large number of runs in order to eliminate fluctuations.

the scaling state: the topological distributions of the bubbles and the survivors did not deviate considerably from the results obtained using model B. One could expect this, because the modification of the rules of model C is important only when one of the neighbors of a rectangle is much larger than the other three. In the scaling regime we do not expect this situation, so the two models are expected to give the same results. Thus we can hope that finally we have a topological model that describes well all known real and numerical experiments on soap froth.

IV. SUMMARY

It has been noticed recently that the traditional topological model (model A), that uses a random choice for the results of T2 processes, exhibits discrepancies with experiments. The disagreement is quite insignificant as long as we measure the topological distribution of the bubbles in the scaling state, but the deviation becomes considerable for some features of the transient behavior [such as the peak of $\mu_2(t)$], for the survivors' topological class distribution and for the cluster grown from a single defect. An attempt to improve the topological model was made in our previous work [9], where a topological model of the soap froth dynamics was suggested (model B). This model differs from model A in that T2 rearrangements are performed with more care than just at random; it turns out that the result of the rearrangement depends on the neighbors of a vanishing bubble.

The way rectangles vanish according to model B has been revised now and a new model C was introduced. We noticed that model B ignored the fact that four-sided bubbles must be perfect rectangles and therefore pairs of opposite sides vanish. We found a way to include this effect in the model within the framework of the topological approach. In fact, this small detail would not play a role, unless the four neighbors of the shrinking rectangle were very different in size. Consequently, model C gives a different result only for the *single cluster growth*. For this problem models A and B gave qualitatively similar results, namely, that the topological distribution of the cluster approaches a fixed form with the second moments $\mu_2^A=0.72$, $\mu_2^B=1.1$. These results disagree with two extensive simulations of the problem that use the Potts model and the model of Weaire and Kermode. Both simulations yield unbounded growth of the second moment of the topological distribution. Model C agrees with these studies, yielding $\mu_2^C(t)\to\infty$ as well.

Thus we must conclude that answers to various questions that go beyond the simplest characteristics of the scaling state are very sensitive to the way T2 processes are performed. We believe that model C introduced in this paper is in good agreement with the experimental data that are available today.

ACKNOWLEDGMENTS

This research was supported by grants from the Germany-Israel Science Foundation (GIF) and by the US-Israel Binational Science Foundation (BSF). B. L. thanks the Clore Foundation for financial support. We thank D. Weaire for most helpful correspondence and J. Stavans for discussions. We are also grateful to H. J. Ruskin and Y. Feng for sending us a copy of their unpublished work.

[1] J. Stavans, Rep. Prog. Phys. **56**, 733 (1993).
[2] C. S. Smith, in *Metal Interfaces*, edited by C. Herring (American Society for Metals, Cleveland, 1952), p. 65.
[3] J. Stavans, Phys. Rev. A **42**, 5049 (1990).
[4] J. Stavans and J. A. Glazier, Phys. Rev. Lett. **62**, 1318 (1989); J. A. Glazier and J. Stavans, Phys. Rev. A **40**, 7398 (1989).
[5] J. A. Glazier, S. P. Gross, and J. Stavans, Phys. Rev. A **36**, 306 (1987).
[6] W. Y. Tam and K. Y. Szeto (unpublished).
[7] J. Von Neumann, *Metal Interfaces*, edited by C. Herring (American Society for Metals, Cleveland, 1952), p. 108.
[8] B. Levitan, E. Slepyan, O. Krichevsky, J. Stavans, and E. Domany, Phys. Rev. Lett. **73**, 756 (1994).
[9] B. Levitan and E. Domany, Europhys. Lett. **32**, 543 (1995).
[10] B. Levitan, Phys. Rev. Lett. **72**, 4057 (1994).
[11] D. Weaire and J. P. Kermode, Philos. Mag. B **48**, 245 (1983).
[12] T. Herdtle and H. Aref, J. Fluid Mech. **241**, 233 (1992).
[13] K. Nakashima, T. Nagai, and K. Kawasaki, J. Stat. Phys. **57**, 759 (1989).
[14] G. S. Grest, M. P. Anderson, and D. J. Srolovitz, Phys. Rev. B **38**, 4752 (1988).
[15] E. A. Holm, J. A. Glazier, D. J. Srolovitz, and G. S. Grest, Phys. Rev. A **43**, 2662 (1991).
[16] J. Wejchert, D. Weaire, and J. P. Kermode, Philos. Mag. B **53**, 15 (1986).
[17] C. W. J. Beenakker, Phys. Rev. A **37**, 1697 (1988).
[18] V. E. Fradkov, L. S. Shvindlerman, and D. G. Udler, Scr. Metal. **19**, 1285 (1985); Philos. Mag. Lett. **55**, 289 (1987).
[19] D. Weaire and H. Lei, Philos. Mag. Lett. **62**, 427 (1990).
[20] Y. Jiang, J. C. M. Mombach, and J. Glazier, Phys. Rev. E **52**, 3333 (1995).
[21] H. J. Ruskin and Y. Feng (unpublished) [see also H. J. Ruskin and Y. Feng, J. Phys. Condens. Matter **7**, L553 (1995)].
[22] M. Marder, Phys. Rev. A **36**, 438 (1987).
[23] V. E. Fradkov, M. O. Magnasco, D. G. Udler, and D. Weaire, Philos. Mag. Lett. **67**, 203 (1993); V. E. Fradkov, M.E. Glickman, J. Nordberg, M. Palmer, and K. Rajan, Physica D **66**, 50 (1993).
[24] Our model is completely deterministic. Runs differed from one another by small random perturbations of the initial areas of the hexagons $[a_i(0)=1+\zeta_i, i=1,\ldots,N$, where ζ_i are small random numbers].
[25] Note that both curves presented in Fig. 3 have peak values that are a bit smaller than the values μ_2^{peak} presented in Fig. 4 for the corresponding values of defect densities c. This is because of the different averaging procedures used for the two plots: the curves presented in Fig. 3 are obtained by the averaging of six runs; each of these achieved its maximum at slightly different times. Hence the average value of μ_2^{peak} is a bit lower than the values presented in Fig. 4, where the peak values themselves were averaged.